Eukaryotic biodiversity and ecological networks from the surface to the mesopelagic in the Northwest Atlantic Slope Water

Nina Yang[1,2], Elizabeth A. Allan[3], Sarah E. Stover[1†], Benjamin D. Grassian[1,4‡], Heidi M. Sosik[1], Joel K. Llopiz[1], Annette F. Govindarajan[1]

[1]Department of Biology, Woods Hole Oceanographic Institution, Woods Hole, MA, USA

[2]Marine Policy Center, Woods Hole Oceanographic Institution, Woods Hole, MA, USA

[3]School of Marine and Environmental Affairs, University of Washington, Seattle, Washington, USA

[4]Department of Applied Ocean Physics and Engineering, Woods Hole Oceanographic Institution, Woods Hole, MA, USA

Correspondence: Nina Yang, nina.yang@whoi.edu

[†]**Present Address:** Graduate School of Biology, University of Vermont, Burlington, Vermont, USA

[‡]**Present Address**: Graduate School of Oceanography, University of Rhode Island, Narragansett, RI, USA

1. ABSTRACT

The diversity and interactions among mesopelagic organisms are difficult to study and as a result, are insufficiently unaccounted for in food web and biogeochemical models. This knowledge gap hinders our ability to model and forecast ecosystem function and formulate effective policies for conservation and management in the face of growing interest in exploiting midwater living resources. We used multi-marker metabarcoding of environmental DNA (eDNA) samples collected from Northwest Atlantic Slope Water to resolve patterns of eukaryotic community composition spanning taxonomically across protists (microbial eukaryotes),

invertebrates, and vertebrates and vertically from the ocean surface to the base of the mesopelagic zone. With statistical network analyses, we explored cross-kingdom associations including trophic interactions such as food web dynamics and evaluated network robustness to biodiversity loss. We found depth-specific communities of distinct protist, invertebrate, and vertebrate assemblages. Ecological networks for the epipelagic, upper mesopelagic, and lower mesopelagic suggest that protists are keystone taxa and important mediators of trophic interactions; they increase network complexity and contribute to network stability. We also identified metazoans including copepods, gelatinous taxa (cnidarians, tunicates), and mesopelagic fish as important components of network interactions. Our study demonstrates a holistic approach to generate insights on mesopelagic biodiversity and implications for ecosystem resilience that can inform future conservation and management efforts.

2. INTRODUCTION

Diverse ecological communities underpin ecosystem function and critical ecosystem services (Oliver et al., 2015; Sala et al., 2021; Nauta and De Domenico, 2024). In the vast mesopelagic region of the ocean from the base of the sunlit zone to 1000 m deep (Buesseler et al., 2020), a wide variety of life supports important hunting grounds for commercially and ecologically relevant fish including sharks, tuna, and billfish (Braun et al., 2023; Iglesias et al., 2023; Willis et al., 2025). This region is also a significant reservoir of organic carbon (Arístegui et al., 2009) and biogeochemical processes that occur at these depths determine flux into deeper waters and subsequent long-term sequestration (Mazuecos et al., 2015; Cavan et al., 2019; Nguyen et al., 2022).

Despite the recognized importance of the deep sea, studies have primarily focused on coastal surface or epipelagic (surface) ecosystems, leaving the mesopelagic both undersampled and understudied (St. John et al., 2016). These knowledge gaps are largely driven by challenges associated with accessing and sampling a vast ecosystem that spans considerable horizontal and vertical spatial scales (Sutton et al., 2017). Difficulty acquiring logistical resources and expertise for deep sea exploration and research are also major contributing factors (Tolochko and Vadrot, 2021; Amon et al., 2022). Furthermore, many studies focus on specific groups of organisms in isolation, such as those exclusively examining microbes or metazoans (Yang et al., 2024), which greatly skews our understanding of biodiversity, ecological interactions, and functional roles.

Environmental DNA (eDNA) approaches have emerged as reliable tools to assess biodiversity at scale (McClenaghan et al., 2020; Chavez et al., 2021; Holman et al., 2021; Yeh and Fuhrman, 2022; Govindarajan et al., 2023a; Dan et al., 2024). Recent studies employing multiple marker metabarcoding approaches resolve diversity patterns across the domains of life – from prokaryotes to top predators (Djurhuus et al., 2020; Holman et al., 2021). Using statistical and network analyses, these studies have documented key predator-prey interactions, identified potential keystone taxa, and uncovered unexplored trophic connections that may serve as

64 indicators of ecosystem function in a changing ocean. As growing interest in mesopelagic
65 fisheries for aquaculture and nutraceuticals (Martin et al., 2020; Bisson et al., 2023) and deep sea
66 mining activities (Drazen et al., 2020) threaten overexploitation and habitat destruction, a more
67 complete understanding of biodiversity and ecological dynamics is needed to inform the
68 sustainable management of mesopelagic resources.

69 Collectively, microbially catalyzed biogeochemical transformations and animal feeding
70 behaviors, including diel vertical migration, are core processes that influence carbon dynamics in
71 the surface and deep ocean. In the epipelagic ocean (~0 m-200 m), phytoplankton harness energy
72 from the sun to convert carbon dioxide into organic carbon. Zooplankton grazing and senescence
73 of primary production can export organic carbon out of the surface ocean, providing a food source
74 for life in the deep ocean (Cawley et al., 2021; Hemsley et al., 2023) and contributing to the largest
75 reservoir of organic carbon on earth (Arístegui et al., 2009). In the mesopelagic, the balance
76 between microbial remineralization of organic carbon to carbon dioxide and assimilation into
77 biomass within the food web impacts carbon flux into deeper waters where carbon can be
78 sequestered for variable time periods (e.g., 10-1000 years) (Mazuecos et al., 2015; Cavan et al.,
79 2019; Nguyen et al., 2022). For these reasons, organismal interactions including food web
80 dynamics in the epipelagic and mesopelagic zones are interconnected and play a determinant
81 role in the fate of carbon in the ocean (Robinson et al., 2010; Herndl and Reinthaler, 2013; Giering
82 et al., 2014).

83 Few multi-marker metabarcoding studies have been conducted in deep pelagic
84 ecosystems and existing studies tend to emphasize organismal diversity and distribution rather
85 than interactions among taxa (Giner et al., 2020; Laroche et al., 2020a; Govindarajan et al., 2021;
86 Holman et al., 2021; Govindarajan et al., 2023b). A more holistic approach would facilitate our
87 ability to effectively understand how community composition and organismal interactions across
88 the tree of life influence crucial ecosystem processes. We aimed to investigate patterns of
89 biodiversity and their interactions to better understand ecosystem structure and stability from the

surface to the base of the mesopelagic in the Northwest Atlantic Slope Water region. We applied an eDNA metabarcoding approach with two markers to resolve the eukaryotic community, inclusive of microeukaryotes (protists), invertebrates, and vertebrates, and calculated diversity indices to determine depth-specific biodiversity patterns. We then performed covariance network analyses on multi-marker metabarcoding data, constructing depth-specific networks for metazoans (invertebrates and vertebrates), protists, and all taxa combined across the epipelagic (10 m, 100 m), upper mesopelagic (300 m, 500 m), and lower mesopelagic (800 m, 1000 m) depth zones.

Network topologies revealed depth-specific trends of network complexity determined by the total number of nodes (ASVs), edges (interactions or links), and link density (edge-to-node ratio) (Landi et al., 2018). We explored the influence of complexity across depth zones on network stability, determined by sequentially removing ASVs from the networks (node connectivity and robustness) and edges (edge connectivity) (Iyer et al., 2013; Tipton et al., 2018). Collectively, these analyses revealed insights on the role of marine protists as keystone taxa, especially at mesopelagic depths. A diverse protistan community contributes to network stability and facilitates a significant proportion of trophic interactions involving invertebrate and vertebrate taxa, suggesting their vital role in food web dynamics and ecosystem resilience.

3. MATERIALS & METHODS

3. 1. Sample Collection

Bulk water samples were collected in Northwest Atlantic Slope Water in March 2020 on the *R/V* Armstrong (AR43) at six discrete depths (10 m, 100 m, 300 m, 500 m, 800 m, and 1000 m) at three sampling stations (Figure 1). Sampling spanned surface depths to the base of the mesopelagic and included the deep scattering layer (~500 m) as determined by a broadband Simrad EK80 split beam echosounder system on the *R/V* Armstrong (Supplementary Figure S1, Supplementary Methods). Water was collected with a 24-Niskin CTD rosette across three casts

at sampling sites with similar water column characteristics (Figure 1). Two casts (001 and 007) were collected at midnight while cast 002 was collected at mid-day. At each depth, four replicates were collected for a total of 72 samples. For each sample, ~5 L of water was pumped through sterile 0.2 µm PES Sterivex (MilliporeSigma, Burlington, MA, USA) filters, sealed with Luer lock caps, and stored at -80°C. Sample collection carboys and filtration tubing were bleach-sterilized and rinsed with Milli-Q water prior to filtration with a Masterflex L/S peristaltic pump system following established protocols (Govindarajan et al., 2021, 2022).

The AR43 expedition coincided with high densities of the salp *Salpa aspera*, gelatinous zooplankton that are known to periodically "bloom" in the Northwest Atlantic Slope Water (Wiebe et al., 1979; Madin et al., 2006). From analysis of in situ high speed (15 Hz) image data, we estimated densities of 5-10 individuals m^{-3} in surface waters at night (Supplementary Figure S2, Supplementary Methods), which are in the typical range for bloom densities (e.g., 3.5 individuals m^{-3} and higher) (Groeneveld et al., 2020).

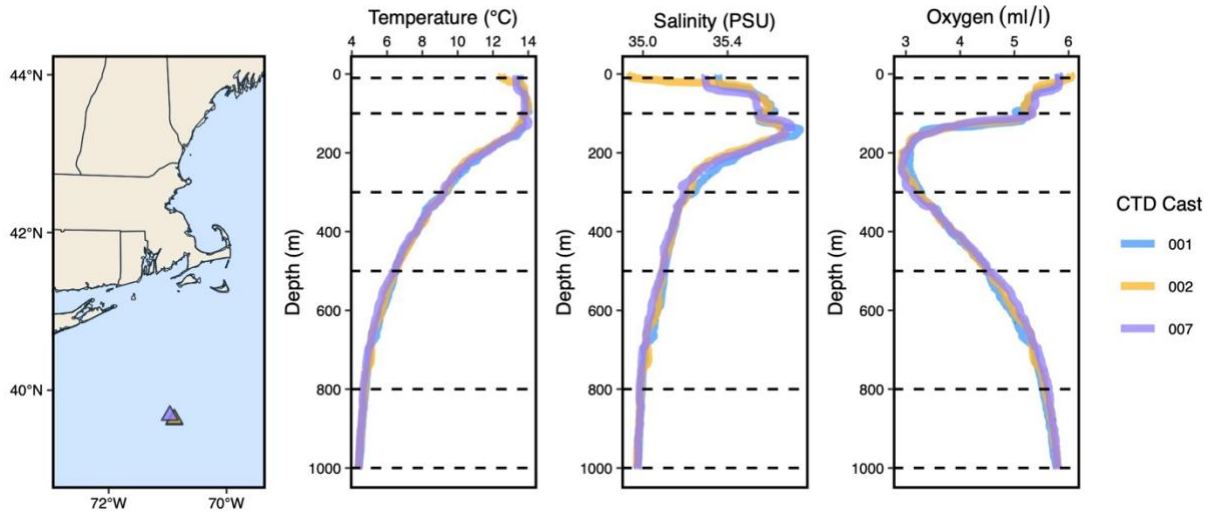

Figure 1. Sampling location and CTD profiles for eDNA collection. Temperature, salinity, and oxygen profiles for each CTD cast (001, 002, and 007) where eDNA samples were collected are shown. Dashed black lines indicate the depths where samples were collected (10 m, 100 m, 300 m, 500 m, 800 m, and 1000 m).

134 **3.2. DNA Extractions and PCR**

135 DNA was extracted with a Qiagen DNEasy Blood & Tissue extraction kit (Qiagen,
136 Germantown, MD, USA) following manufacturer's protocols with modifications for Sterivex filters
137 (Govindarajan et al., 2021). Extracted DNA was stored at -20°C prior to metabarcoding. All
138 samples were metabarcoded for portions of the 18S and 12S rRNA genes (see below), except
139 for one sample collected on CTD cast 007 at 1000 m which did not have enough DNA template
140 for 12S rRNA metabarcoding. All lab surfaces and equipment were cleaned with a 10% sodium
141 hypochlorite solution (household bleach) and extractions were performed in a dedicated
142 laboratory space away from sources of concentrated DNA such as post-PCR or tissue samples.

143 The 18S V9 hypervariable region was amplified using the 1380F/1510R primer set with
144 CS1/CS2 Fluidigm adapters and following a two-step PCR protocol (Amaral-Zettler et al., 2009;
145 Govindarajan et al., 2021). The initial PCR cycling program began with a denaturation step at
146 95°C for 3 min, 25 cycles at 95°C for 30 sec, 55°C for 30 sec, and 72°C for 30 sec, followed by
147 an elongation step at 72°C for 5 min. PCR reactions (25 µl) consisted of 2.5 µl of DNA template,
148 0.5 µl of each primer, 12.5 µl of 2x KAPA HiFi HotStart ReadyMix (Kapa Biosystems; Wilmington,
149 MA, USA), and 9 µl of molecular-grade water. Duplicate PCR reactions were run for each sample,
150 pooled, and sent to the Genome Research Core at the University of Illinois at Chicago (UIC) to
151 complete a second PCR amplification to add unique tags using MyTaq HS 2X Master Mix and the
152 Access Array Barcode Library for Illumina (Fluidigm, South San Francisco, CA, USA). The PCR
153 cycling program was as follows: 95°C for 5 min followed by 18 cycles of 95°C for 30 sec, 60°C for
154 30 sec, 72°C for 30 sec, and 72°C for 7 min. Amplicon libraries were purified using AMPure XP
155 beads (Beckman Coulter, Indianapolis, IN, USA). Amplicon sequencing with a targeted
156 sequencing depth of 100000 reads per sample was done on an Illumina MiSeq (2x250 bp)
157 (Govindarajan et al., 2022).

158 The hypervariable 12S region of the mitochondrial rRNA gene was amplified using MiFish
159 primers (Miya et al., 2015) appended with Illumina adapter overhang nucleotide sequences and

160 a modified two-step PCR protocol with a touch-down PCR program for the first PCR (Pitz et al.,
161 2020). The initial PCR cycling program began with a denaturation step at 95°C for 15 min; 13
162 cycles of 94°C for 30 sec, 69.5°C for 30 sec (decreasing 1.5°C with each cycle), and 72°C for 90
163 sec; 25 cycles of 94°C for 30 sec, 50°C for 30 sec, and 72°C for 45 sec; followed by an elongation
164 step at 72 °C for 10 min. PCR reactions (25 µl) consisted of 2.5 µl of DNA template, 1 µl of each
165 primer, 12.5 µl of 2x KAPA HiFi HotStart ReadyMix, and 8 µl of molecular-grade water. Duplicate
166 PCR products were pooled and sent to the Center for Genome Innovation at the University of
167 Connecticut for size selection, a second round of PCR, and sequencing. Amplicons from the
168 pooled PCR products were visualized with the Agilent 4200 TapeStation electrophoresis system
169 using the High Sensitivity DNA D1000 assay (Agilent Technologies, Santa Clara, CA). Size-
170 selection for targeted amplicons (215bp-335bp) was conducted using the Sage Science
171 PippinPrep HT gel cassette (2% Agarose, PippinHT). Illumina barcodes were added to each
172 amplicon using a second PCR amplification. The PCR cycling program was as follows: 95°C for
173 3 min followed by 12 cycles of 95°C for 15 sec, 60°C for 30 sec, and 72°C for 90 sec. Amplicon
174 libraries were purified using AMPure XP beads and assessed for quality and adapter dimer
175 content on the Agilent 4200 TapeStation using a D1000 assay. Amplicon sequencing with a
176 targeted sequencing depth of 100000 reads per sample was done on an Illumina MiSeq
177 (2x250bp) with 20–30% PhiX added (Illumina, San Diego, CA).
178 For both 18S and 12S primer sets, PCR runs included field controls of filtered Milli-Q water
179 (1 L for each CTD cast) as well as PCR negative (without DNA template) and positive controls.
180 The PCR positive control was included to determine the quality of sequencing results and
181 consisted of previously extracted 1ng/µl sample of *Fundulus heteroclitus*, an estuarine fish that
182 would not be found in the environmental samples.
183
184 **3.3 Multi-marker metabarcoding bioinformatics**

185 Demultiplexed sequencing reads were imported into and processed in QIIME 2 with
186 default settings (v2022.11.1) (Bolyen et al., 2019). Adapters and primers were trimmed from the
187 reads with Cutadapt (Martin, 2011). Reads were quality-filtered, trimmed to the primer region 120
188 bp (18S) and 150 bp (12S), denoised, and merged into amplicon sequence variants (ASVs) with
189 DADA2 (Callahan et al., 2016). For both gene markers, taxonomy was assigned by a naïve Bayes
190 classifier at an 80% confidence threshold (Pedregosa et al., 2011); the classifier was trained on
191 reference databases curated and evaluated with the REference Sequence annotation and
192 CuRatIon Pipeline (RESCRIPt) QIIME 2 plugin (Robeson et al., 2021).
193 The 18S sequencing reads were annotated with two different databases: one for protists
194 and one for metazoans. The protist (18S) classifier was trained with the Protistan Ribosomal
195 Reference (PR2) database (v5.0.1) (Guillou et al., 2013) that was updated with 9 taxonomic levels
196 including the replacement of kingdom with domain and the addition of a new subdivision level.
197 The metazoan (18S) classifier was trained with the SILVA SSURef_NR99 (v138.1) database
198 (Pruesse et al., 2007; Quast et al., 2013). A new 12S classifier was created by combining a
199 custom reference database of 12S sequences for 80 species of mesopelagic fish from the
200 Northwest Atlantic (Govindarajan et al., 2023b) with the MetaZooGene database (v2023-m07-15)
201 in Mode-A (most inclusive option) for vertebrates (O'Brien et al., 2024). For 18S sequences,
202 taxonomy assignments were first assigned with PR2 and protist sequences were selected as the
203 subset where phylum was not classified as "Metazoa". This subset will be referred to as the protist
204 dataset. Sequences where phylum was classified as "Metazoa" were subsequently classified with
205 the SILVA-based classifier. Metazoan 18S reads were classified predominantly as invertebrate
206 taxa and will be referred to as the invertebrate dataset (Govindarajan et al., 2021). Likewise,
207 metazoan 12S reads were classified as vertebrates (mainly fish) and will be referred to as the
208 vertebrate dataset. For downstream bioinformatic and statistical analyses, the 18S reads were
209 processed separately as two individual datasets representing protist and invertebrate reads, while
210 12S reads represented the standalone vertebrate dataset.

211 After taxonomic classification, 142 of 399 invertebrate ASVs remained unassigned at the
212 phylum level or were unassigned sequences from the phylum Arthropoda, which represented
213 18.4% of all sequences in the invertebrate dataset. Of those 142 ASVs, one ASV represented
214 ~13% of invertebrate reads and comprised of ~48% of reads at 100 m (Supplementary Figure
215 S3A). These unassigned sequences were manually classified with Geneious Prime 2025.0.3 with
216 a BLAST search and NCBI's new BLAST core nucleotide database (core_nt). The top match was
217 selected from the assigned grade score at a 95% cut-off. This approach annotated 67 of the 142
218 unassigned invertebrate ASVs, which reduced the total number of unassigned reads to 0.35%.
219 Most unassigned reads were classified to Order Calanoida (calanoid copepods). Similarly, 345 of
220 677 vertebrate ASVs remained unassigned with > 80% of ASVs classified as Unassigned
221 Actinopterygii (ray-finned fishes). Altogether, unassigned ASVs comprised 12.9% of reads.
222 Following the BLAST process described for invertebrates, 117 vertebrate ASVs were successfully
223 classified, reducing the unassigned read percentage to ~1% (Supplementary Figure S3B).
224 Taxonomy, ASV count, and metadata files were imported into R (v4.3.2) with qiime2R
225 (v0.99.6) (https://github.com/jbisanz/qiime2R) and merged with phyloseq (v1.46.0) (McMurdie
226 and Holmes, 2013) to generate phyloseq objects for protists, invertebrates, and vertebrates.
227 Potential contaminants were identified and removed with the R package decontam and a
228 conservative threshold of 0.5, which identifies all sequences more prevalent in negative controls
229 than samples as contaminants (Davis et al., 2018). In total, decontam identified and removed 44
230 protist, 19 invertebrate, and 17 vertebrate ASVs. Additional decontamination of the datasets was
231 conducted manually and detailed in Supplementary Methods. Samples with less than 15000
232 reads (protists), 6000 reads (invertebrates), and 3000 reads (vertebrates) were removed,
233 resulting in 69 samples (protists), 70 samples (invertebrates), and 61 samples (vertebrates) out
234 of 72 total samples.
235 Alpha diversity indices (richness, Shannon Index, evenness) were calculated from a
236 rarefaction approach with iterative subsampling (1000 iterations) and a subsampling threshold

determined by the minimum read count of 27865 (protists), 6076 (invertebrates), and 3183 (vertebrates) in the sample set (Schloss, 2024). Diversity indices reflect the mean index value for each depth after rarefaction and statistical significance was computed by one-way ANOVA with Tukey's HSD post-hoc analysis (p value < 0.05).

Depth-specific community composition was assessed with principal component analyses conducted with the rda function in vegan v2.6.4 (Oksanen et al., 2022) on centered log-ratio (CLR) transformed ASV counts (Aitchson, 1986; Coenen et al., 2020). Zero-value data were replaced with the "const" method which replaces zeros with 65% of the next lowest value (Bastiaanssen et al., 2022). Statistical significance was determined with permutational multivariate analysis of variance (PERMANOVA) with the adonis2 function in vegan on Euclidean distance matrices. Pairwise comparisons were conducted with the pairwise.adonis2 function from the pairwiseAdonis package v0.4 (Arbizu, 2020). ASVs were grouped into relevant taxonomic groups of ecological and functional significance for taxa bar plots to show the proportion of ASV composition and relative abundance. UpSet plots were used to visualize ASV overlap across depths, with a matrix format that shows which ASVs are shared or unique to specific depths. Taxa with low relative abundance (< 1%) were grouped to streamline visualizations with additional details provided in Supplementary Materials (Supplementary Tables S1-S3).

3.4 Network Analyses

Network analysis from Sparse InversE Covariance Estimation for Ecological Association inference (SPIEC-EASI) was applied to protist, invertebrate, and vertebrate compositional datasets to assess ASV-ASV co-occurrence patterns with depth across these datasets (Kurtz et al., 2015; Tipton et al., 2018). SPIEC-EASI identifies statistically significant relationships while accounting for issues inherent to compositional metabarcoding datasets (Kurtz et al., 2015). ASV count tables are CLR-transformed and a graphical model inference framework is used to identify

262 direct associations between ASVs while minimizing indirect correlations and reducing the
263 detection of spurious relationships.

264 Samples were grouped into three depth zones: epipelagic (10 m and 100 m), upper
265 mesopelagic (300 m and 500 m), and lower mesopelagic (800 m and 1000 m). Out of a possible
266 total of 24 samples in each depth zone, only samples that contained protist, invertebrate, and
267 vertebrate ASVs were retained for network analysis, resulting in a total of 15 epipelagic samples,
268 21 upper mesopelagic samples, and 22 lower mesopelagic samples. ASVs were filtered on
269 abundance (> 50 reads) and prevalence (present in at least 10% of samples in each depth zone)
270 to minimize dense networks and focus the analyses on prevalent and abundant ASVs.

271 Undirected networks were generated for each depth zone for metazoan-only (invertebrate
272 and vertebrate) ASVs, protist-only ASVs, and all ASVs (All Taxa) for a total of nine networks. In
273 each network, edges (links) represent signed associations (positive or negative) between nodes
274 (ASVs). The SpiecEasi v1.1.1 package was used to construct these networks on WHOI's high-
275 performance computing cluster in R v4.4.3, applying the Meinshausen–Buhlmann's neighborhood
276 selection method with an optimal sparsity threshold (lambda min ratio) of 1e-3, and 100
277 subsampling replicates (rep.num = 100) (Kurtz et al., 2015). Networks were then exported into
278 RStudio to assess network topology and robustness with igraph v2.0.2 in R (Csárdi and Nepusz,
279 2006).

280 Although ecological networks can be built from species-level or other taxonomic groups,
281 we built networks from ASVs, the lowest genetic unit, to render an appropriate comparison across
282 the three datasets generated from two markers of varying taxonomic resolution. For example,
283 18S V9 reliably resolves taxonomy to the order level while 12S MiFish can resolve to species
284 level. To show this, we evaluated the three naïve Bayes classifiers referenced in this study with
285 the evaluate-fit-classifier function in the QIIME 2 RESCRIPt plugin (Robeson et al., 2021) to test
286 the classifiers' performance on the same sequences it was trained with. The F-measure score,
287 which reflects the balance between precision and recall, for the 18S V9 classifiers drops below

288 ~0.95 after Order while the 12S classifier has a high F-measure up to species-level classification
289 (Supplementary Figure S4). After networks were generated, ASVs were grouped into relevant
290 taxonomic groups of ecological and functional significance for downstream network analyses.
291
292 **3.5 Visualizations**
293 Unless otherwise specified, figures were generated with ggplot2 v3.5.1 (Wickham, 2016).
294 UpSet plots were generated with ComplexUpset v1.3.3. Networks were visualized with ggnetwork
295 v0.5.13 (Tyner et al., 2017). When necessary, visualizations were compiled with minimal editing
296 for aesthetics with the creative software, Affinity Designer 2 (Serif, Europe).
297
298 **4. RESULTS**
299 **4.1 Patterns of diversity from 18S and 12S metabarcoding**
300 Metabarcoding of the 18S V9 rRNA gene generated ASVs for protists and invertebrates
301 while the 12S MiFish metabarcoding generated ASVs for vertebrates (predominately fish). The
302 18S dataset ranged from 70-90% protist sequences with the proportion of invertebrate sequences
303 decreasing with depth (Supplementary Figure S5). Protist and invertebrate sequences were
304 parsed from the 18S dataset and assessed separately. Following decontamination and rarefaction
305 of metabarcoding reads, a total of 8112 ASVs were recovered across both markers with 7046
306 (86.9%) for protists, 399 (4.9%) for invertebrates, and 667 (8.2%) for vertebrates. The numbers
307 of observed ASVs (or ASV richness) for protists and invertebrates were generally higher in the
308 mesopelagic than the epipelagic with relatively constant richness across mesopelagic depths
309 (Figure 2). For vertebrates, higher richness was observed at 10 m and 500 m than at other depths.
310 For invertebrates, Shannon diversity indices were significantly different between surface (10 m)
311 and all other depths ($p < 0.01$) while Pielou's evenness indices varied significantly at depth,
312 especially between 100 m and select mesopelagic depths ($p < 0.05$). For vertebrates, average
313 Shannon and Pielou's indices followed similar patterns as observed for ASV richness, although

no significant differences were observed between depths (Supplementary Tables S4-S6). For protists however, Shannon and Pielou indices exhibited patterns that contrasted with those for richness. The highest Shannon diversity and Pielou evenness indices occurred at 100 m and then decreased with depth down to 500 m before increasing again to 1000 m.

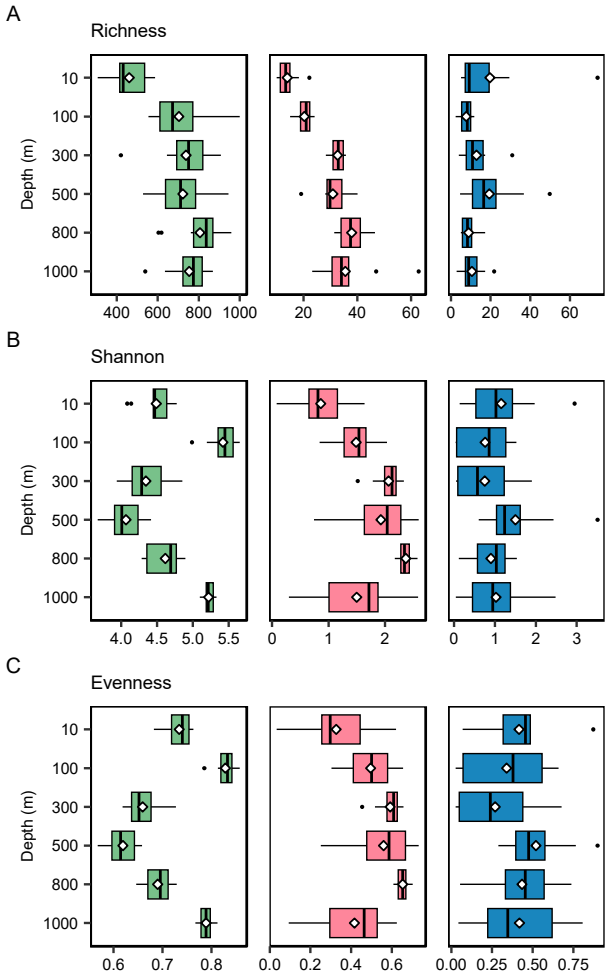

Figure 2. Patterns of alpha diversity with depth for A) Richness (observed ASVs), B) Shannon Diversity Index, and C) Pielou's Evenness Index across all samples for protists (n=69), invertebrates (n=70), and vertebrates (n=61). Boxplots show the variation in diversity indices at each depth between samples divided into quartiles with outlier values indicated by black points. A white diamond indicates the mean value at each depth.

Protistan diversity in epipelagic waters was comprised of mostly alveolates (dinoflagellates, Syndiniales, and ciliates) and stramenopiles (e.g., diatoms) (Supplementary Figure S6A). Alveolate ASVs increased in mesopelagic waters, as did rhizarian (e.g., radiolarians) and excavate ASVs, with these three groups representing a significant portion of protistan

329 diversity (Supplementary Figure S6D). Invertebrate diversity was driven mainly by taxonomic
330 groups with relative read abundance < 1% (rare reads), including Trachymedusae and
331 Narcomedusae (Cnidaria) (Supplementary Figure S6B, Supplementary Table S2). Orders
332 Calanoida (calanoid copepods) and Siphonophorae (Cnidaria; siphonophores), as well as
333 unassigned metazoan ASVs, also represented a significant portion of diversity (Supplementary
334 Figure S6E). Fish were the main category of vertebrate ASVs detected (Supplementary Figure
335 S6C), with a significant portion attributed to deep sea fish taxa including Melamphidae (bigscales),
336 Myctophidae (lanternfish), and Gonostomatidae (bristlemouths). Similar to the invertebrates, rare
337 taxonomic groups (low read count) contributed significantly to vertebrate diversity (Supplementary
338 Figure S6F). Five mammalian ASVs were also detected, comprising ~0.038% of the total dataset.
339 These included ASVs assigned to whales and dolphins known to occur at the study site, including
340 two ASVs from the genus *Balaenoptera* (whales) and three ASVs for dolphins in the genera
341 *Delphinus*, *Stenella*, and *Grampus* (Supplementary Table S3).
342
343 **4.2 Depth structuring of the eukaryotic community**
344 Principal component analysis (PCA) and PERMANOVA of rarefied, center-log ratio (CLR)
345 transformed protist and invertebrate reads from all samples revealed significant depth clustering
346 ($p < 0.001$) (Figure 3). Moreover, pairwise comparison showed that communities at each depth
347 were significantly different from other depths ($p < 0.001$). For vertebrate communities, significant
348 differences were observed between surface (10 m) and mesopelagic depths ($p < 0.01$).
349 Differences were also found between 500 m and all other depths ($p < 0.05$). Clustering by CTD
350 cast, which reflected the time of sampling, was not statistically significant ($p > 0.05$). Given the
351 lack of significant diel patterns in this dataset, samples across all three casts were combined at
352 each depth for subsequent analyses.

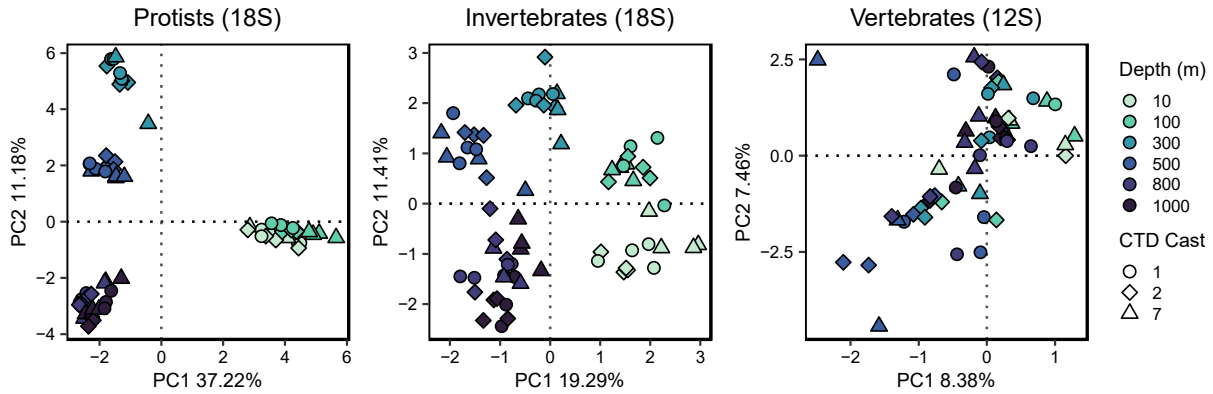

Figure 3. Principal component analysis (PCA) of center-log ratio-transformed reads for protists (n=69), invertebrates (n=70), and vertebrates (n=60). Each point represents one sample. The shape and color of each point indicates the CTD cast and the sampling depth, respectively, of each sample. CTD cast here can also reflect diel sampling with casts 1 and 7 sampled at midnight and cast 2 sampled during mid-day. One outlier (10 m, PC1 = ~10) from the vertebrate dataset was removed for visualization purposes (see Supplementary Figure S7).

Sequenced reads were aggregated by depth to generate relative abundance profiles that reflect the overall water column community structure (Figure 4). For protists, epipelagic (< 200 m) community structure was dominated by photosynthetic taxa including dinoflagellates, diatoms and other stramenopiles, and chlorophytes. The relative abundance of the parasitic taxon Syndiniales, as well as radiolarians, increased with depth and were the dominant taxa in the mesopelagic (> 200 m). Excavates were also relatively more abundant in deeper waters. For invertebrates, calanoid copepods (Arthropoda) exhibited higher relative abundance in both the epipelagic and lower mesopelagic (1000 m), while siphonophores (Cnidaria) were also relatively abundant, especially in the upper mesopelagic. At surface depths, salps were relatively abundant compared to other invertebrate taxa.

Key taxonomic groups were comprised of ASVs that were only detected at one specific depth (unique ASVs), detected at two or more depths (shared ASVs), or detected at all depths (cosmopolitan ASVs) (Supplementary Figure S8). Unique, shared, and cosmopolitan protist ASVs included a mix of both photosynthetic and non-photosynthetic taxa across all depths with deeper waters harboring a higher number of unique ASVs than near the surface (10 m). Unique invertebrate ASVs were greater at mesopelagic depths and dominated by taxa with low relative

abundance (< 1%), while unique vertebrate ASVs were highest at 10 m and 500 m. Across the three organismal groups, unique ASVs were proportionally higher than shared and cosmopolitan ASVs, especially for invertebrates (68.4%) and vertebrates (89.2%) compared to protists (56.6%).

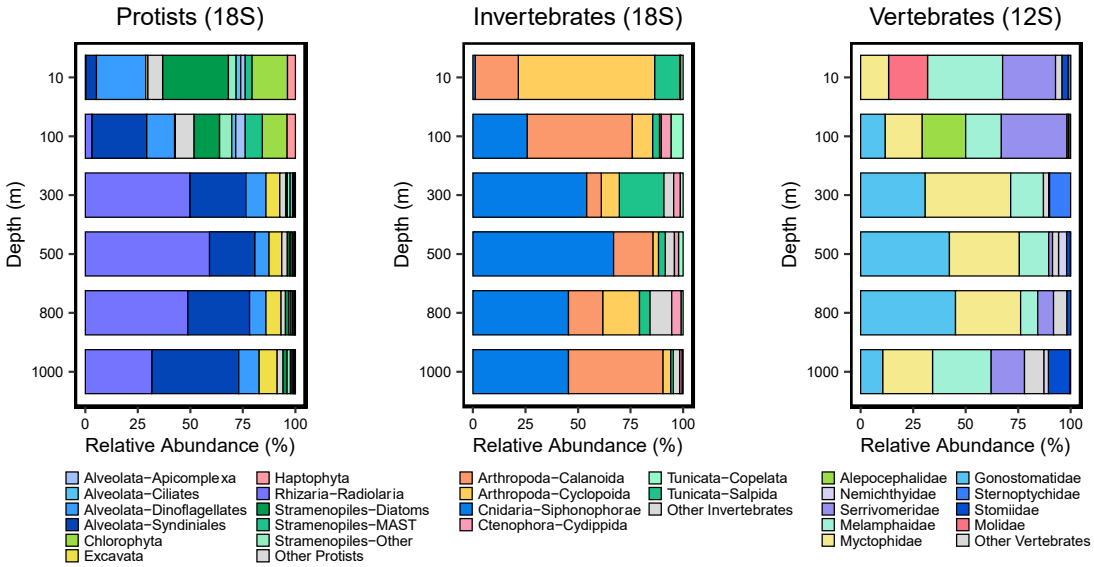

Figure 4. Depth profiles of relative read abundance (%) for protists, invertebrates, and vertebrates calculated from samples aggregated across three CTD casts. Bar plots show taxonomic groups in the order of decreasing relative abundance. In the legend, taxonomic groups within protists (Supergroup and/or Division or Subdivision) and invertebrates (Phylum and Order) are colored and listed in alphabetical order. Vertebrate families were grouped at the Order level in alphabetical order: Alepocephalidae (Alepocephaliformes); Nemichthyidae, Serrivomeridae (Anguilliformes); Melamphidae (Beryciformes); Myctophidae (Myctophiformes); Gonostomatidae, Sternoptychidae, Stomiidae (Stomiiformes); and Molidae (Tetraodontiformes). For each group, only taxa with overall relative abundance > 1% are displayed, with all other taxa combined in "Other". For a full list of "Other" taxa, see Supplementary Tables S1-S3.

Shared and cosmopolitan ASVs for invertebrates and vertebrates may signal animal migration behaviors throughout the water column. For invertebrates, shared and cosmopolitan ASVs included representatives from Orders Calanoida (Arthropoda), Siphonophorae (Cnidaria), Cydippida (Ctenophora), as well as Copelata and Salpida (Tunicata) (Supplementary Figure S9). For vertebrates (Supplementary Figure S10), shared and cosmopolitan ASVs were observed from mesopelagic fish species including *Benthosema glaciale* (Myctophidae), *Cyclothone microdon*,

398 (Gonostomatidae), *Scopeloberyx opisthopterus* (Melamphaidae), and *Serrivomer beanii*
399 (Serrivomeridae).
400
401 **4.3 Depth-specific eukaryotic networks**
402 We generated single-taxon and multi-trophic networks of protists, invertebrates, and
403 vertebrates for the epipelagic (10 m and 100 m), upper mesopelagic (300 m and 500 m), and
404 lower mesopelagic (800 m and 1000 m). Associations between "Metazoa-only" (invertebrates and
405 vertebrates), "Protists-only", and All Taxa (all groups) for each depth zone were inferred with
406 SPIEC-EASI to assess the contribution of broad eukaryotic groups to network connectivity and
407 stability.
408 Metazoa-only networks were small and fragmented, consisting of multiple components
409 including singleton and doubleton associations that resulted in lower complexity networks
410 compared to Protist-only and All Taxa networks (Figure 5, Supplementary Table S7). In contrast,
411 Protist-only networks and All Taxa networks were fully connected such that a link existed between
412 any two nodes in the network. Across all networks, the epipelagic had lower complexity (fewer
413 nodes and edges) and decreased edge density (edge-to-node ratio) compared to the mesopelagic
414 depths.
415 For each network, we assessed resilience and stability to the loss of ASVs (genetic
416 diversity). Node and edge connectivity, the minimum threshold for node or edge removal that
417 fragments a connected network, increased with depth for All Taxa networks (Supplementary
418 Table S7). The lower mesopelagic had the highest threshold for node and edge connectivity for
419 both All Taxa and Protist networks. For the already fragmented Metazoa-only networks,
420 connectivity was zero across all depth zones. We evaluated attack robustness, which measures
421 the size of the network (remaining subnetwork) as nodes are sequentially removed based on
422 betweenness (putative bottlenecks or keystone taxa), degree (highly connected ASVs or hubs),
423 and at random (Iyer et al., 2013; Tipton et al., 2018). Metazoa-only networks were the least robust,

especially in the mesopelagic. Protists-only and All Taxa networks had comparable robustness with higher robustness in mesopelagic networks (Supplementary Figure S11).

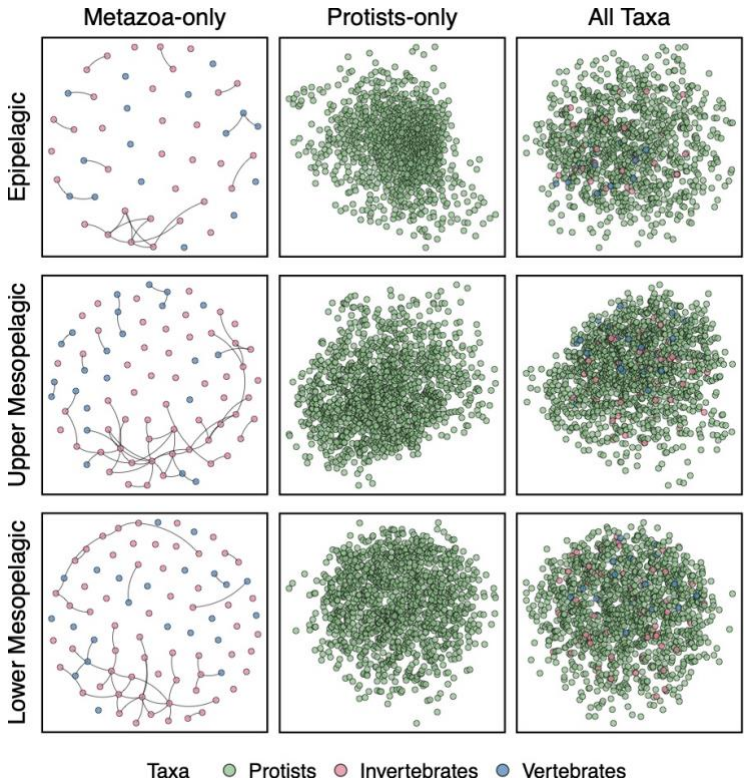

Figure 5. Depth-specific networks for Metazoa-only (invertebrate and vertebrates), Protists-only, and All Taxa (all ASVs). All nodes are shown as points with color indicating the broad taxonomic classification of protists, invertebrates, and vertebrates. Edges are shown for the Metazoa-only network to show the fragmented nature of the network with singleton nodes. The Protists-only and All Taxa networks are connected networks and edges are not shown. All networks include predicted positive and negative interactions.

4.4 Ecological interactions from the surface to the mesopelagic

Positive and negative interactions were separated from the combined networks to explore ecological interactions, especially trophic dynamics across depth. Epipelagic and upper mesopelagic networks averaged 58 and 57% positive interactions, respectively, while the lower mesopelagic network was 53% positive (Supplementary Table S8). On average, the edge density of positive networks was 8.1 compared to 6.5 for negative networks, suggesting that positive networks are more complex. Nodes were compartmentalized into modules that delineated subsets of ASVs that interact more frequently or have stronger interactions than with other ASVs

442 (modularity). Average modularity across the three depth zones was higher for positive networks
443 compared to negative networks (Supplementary Table S9). For both positive and negative
444 networks, modularity decreased with depth. Node and edge connectivity for negative networks
445 averaged 1.33 compared to an average of 2.67 for positive networks. Negative networks were
446 also less robust than positive networks, especially in the epipelagic networks (Supplementary
447 Figure S12).

448 Nodes with the highest edge weights (90th percentile), indicating the strongest interactions,
449 were isolated from the positive and negative networks to explore key ASV associations in each
450 network (Supplementary Figure S13). In both positive and negative subnetworks, the top ranking
451 ASVs based on node degree (number of connections) and betweenness centrality were
452 predominantly protistan taxa, especially Syndiniales (Alveolata) (Supplementary Figures S14-
453 S15). Top ranking invertebrate ASVs included copepods (both calanoid and cyclopoid),
454 siphonophores (cnidarians), and ctenophores while vertebrate ASVs included mesopelagic fish.
455 Notably, *Grampus griseus* (Risso's dolphin) was a top-ranking ASV in the positive network, while
456 salps (tunicates) and *Coryphaena hippurus* (common dolphinfish) were high-ranking ASVs in the
457 negative network.

458 Trophic interactions were assessed by assuming a simple food web from the negative
459 network where protists are at the bottom, invertebrates are intermediate, and vertebrates are top
460 predators. In general, the total number of pair-wise associations (protist-invertebrate, protist-
461 vertebrate, and invertebrate-vertebrate) were highest in the mesopelagic, with 1193 and 1088
462 associations in the upper and lower mesopelagic, respectively, compared to 582 associations in
463 the epipelagic (Figure 6). We narrowed focus to the strongest interactions at each depth zone by
464 selecting ASV-ASV associations with the top 10% of edge weights. Many of these strongest
465 relationships featured protist associations with both invertebrates and vertebrates and highlighted
466 known interactions such as zooplankton grazing of phytoplankton, predator-prey dynamics

between zooplankton and mesopelagic fish, as well as putative parasitic interactions between alveolates and various metazoans (Figure 6).

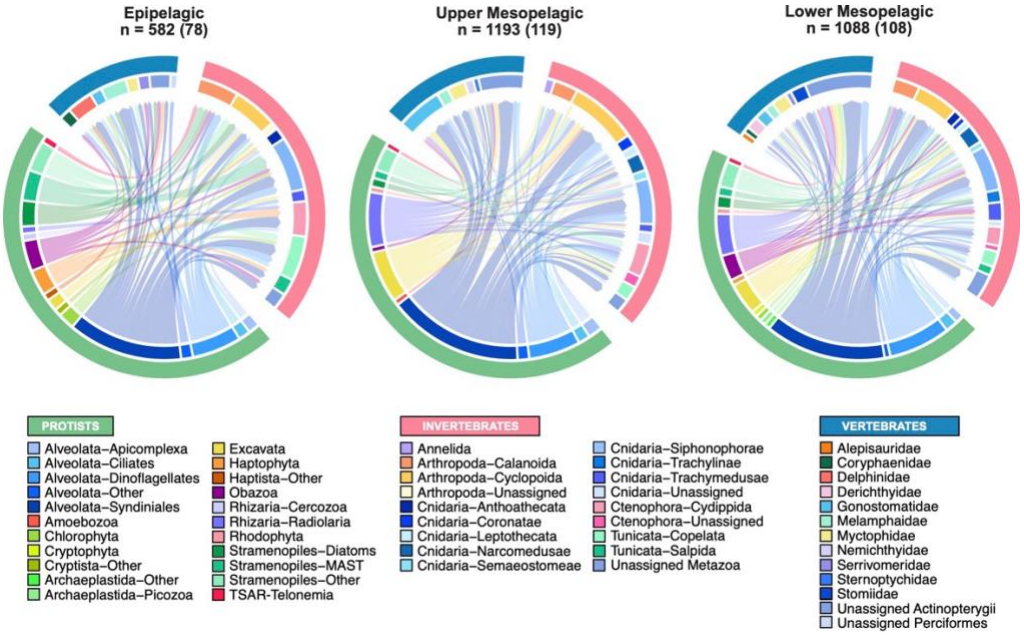

Figure 6. Chord diagrams indicate the number of strong pairwise interactions in the negative network and the taxonomic groups involved at each depth zone. Interactions were selected by removing all ASV-ASV linkages below the 90th percentile threshold for edge weight (so that only the strongest interactions remained). Only protist-invertebrate, protist-vertebrate, and invertebrate-vertebrate interactions were considered. The total number of pairwise associations for each negative network is listed (n) with the number of strong associations in parentheses. Colors along the circumference (track) of the diagram indicate taxonomic groupings. The outer track shows protists in green, invertebrates in pink, and vertebrates in blue. The inner track further divides these taxa into broad functional groups. Each link between two ASVs (or interaction) is depicted as a directional arrow that starts from the ASV in a lower trophic level and points towards the ASV at the higher trophic level. The arrows are also colored based on the lower trophic level ASV. Trophic levels are simplified and ordered as protist > invertebrate > vertebrate. The size of each inner track segment indicates the relative number of ASVs under each functional group within a chord diagram.

5. DISCUSSION

5.1 Protists and metazoans exhibit contrasting diversity patterns

Based on current knowledge of the deep sea, we lack consensus on broad diversity trends due to prevailing gaps across spatial, temporal, and taxonomic scales (Haddock and Choy, 2024; Yang et al., 2024). Traditional midwater assessments often rely on net-based trawls, which sample few depths and regions and can underrepresent taxa that avoid capture or are too fragile

(Kaartvedt et al., 2012; Gold et al., 2021; Suarez-Bregua et al., 2022). As such, deep sea studies that span the eukaryotic community from microeukaryotes to metazoans remain scarce. Since we applied multi-marker metabarcoding to eDNA, this study has generated new insights into eukaryotic biodiversity and ecology from the surface down to the base of the mesopelagic.

A key finding of our study is that alpha diversity increased in the mesopelagic compared to the epipelagic. We found this for both genetic diversity (ASV richness) and Shannon diversity in the Northwest Atlantic Slope Water, especially for protists and invertebrates. This observation counters the existing perspective of decreasing diversity in midwater ecosystems compared to epipelagic waters generated from the global Ocean Biodiversity Information System (OBIS) database (Costello and Chaudhary, 2017). However, Costello and Chaudhary did note a diversity maximum at ~400-500 m, which aligns with our findings, especially for vertebrates (Figure 2). A recent survey of more than two decades of ROV-generated data revealed taxa-specific patterns in the eastern North Pacific such as higher species richness for crustaceans and fishes in the mesopelagic compared to the epipelagic (Haddock and Choy, 2024).

While our findings generally show increasing alpha diversity with depth (Figure 2), we observed low indices for protists between 300 m and 800 m with a minimum at 500 m. We attributed the lower diversity in this depth zone to a small number of ASVs associated with Syndiniales (Dinoflagellata) and Radiolaria (Rhizaria) that are highly abundant relative to other ASVs (Supplementary Figure S14). Through the upper mesopelagic, this trend is generally in line with previous studies that reported a protist diversity maximum at the base of the euphotic zone followed by decreasing diversity in the mesopelagic (Laroche et al., 2020b; Blanco-Bercial et al., 2022). In contrast, other studies have found increasing diversity in the mesopelagic, which we also observed in our dataset at 1000 m (Giner et al., 2020; Ollison et al., 2021).

We also found higher richness in the mesopelagic for invertebrates, which is similar to diversity metrics reported for other areas of the North Pacific (Matthews and Blanco-Bercial, 2023) as well as the southeast Pacific (González et al., 2023), but contrasting with diversity patterns

517 reported off Hawaii (Laroche et al., 2020b). These studies showed that arthropods (especially
518 copepods) and cnidarians are significant contributors to metazoan diversity. In addition, we found
519 vertebrate diversity assessed with the 12S biomarker detected mainly fish. As with previous
520 studies (Canals et al., 2021; Govindarajan et al., 2023b), a significant portion of sequencing reads
521 were associated with deep sea fish (Supplementary Figure S6).

522 For invertebrates and vertebrates, Shannon diversity was high across mesopelagic depths
523 with the highest ASV richness at 500 m for vertebrates, which corresponded with the deep
524 scattering layer detected at 38 kHz (Supplementary Figure S1), a region of the midwater with
525 strong acoustic backscatter from mesopelagic fish and invertebrates (Barham, 1966; Aksnes et
526 al., 2017). Taxonomic groups with low relative abundance (< 1%) or "rare" taxa typically
527 contributed significantly to alpha diversity for protists, invertebrates, and vertebrates
528 (Supplementary Figure S6 and S8). While our study was not explicitly focused on the role of these
529 low abundance taxa, these rare taxa may exert considerable influence over ecosystem function
530 and stability (Lyons et al., 2005; Mouillot et al., 2013; Logares et al., 2014; Lynch and Neufeld,
531 2015; Jousset et al., 2017).

532 There are various factors that may contribute to some of the differences reported across
533 metabarcoding studies. There are differences in methodology (e.g., primer selection, volume
534 filtered, filter pore size or size fractionation, and number of samples), as well as study site (e.g.,
535 Atlantic or Pacific) and seasonal timing of sampling linked to varied environmental conditions that
536 shape the community (Govindarajan et al., 2023a). For example, our study was conducted in the
537 productive Northwest Atlantic Slope Water region and consisted of bulk water sampling (no size
538 fractionation) in March 2020, while the Blanco-Bercial et al. study (2022) was conducted monthly
539 over the course of one year and the Giner et al. study (2020) used size-fractionated water samples
540 (0.2-3 μm).

541 Moreover, the chance encounter of a salp bloom during our sampling (see Methods)
542 contributed to high relative abundance of salp sequences in surface waters (Figure 4) compared

to other studies (Govindarajan et al., 2022; González et al., 2023; Matthews and Blanco-Bercial, 2023). Although we were unable to sample outside of the bloom to assess their impact on community composition, it is possible that diversity trends we observed may have been influenced by high salp densities. For example, previous studies suggest that salp blooms may impact biodiversity by substantially reducing phytoplankton biomass (Zeldis et al., 1995; Décima et al., 2023) and outcompeting other planktonic organisms for food (Paffenhöfer et al., 1995; Perissinotto and A. Pakhomov, 1998; Stukel et al., 2021).

Going forward, the maturation of multi-marker metabarcoding for deep sea studies will benefit from improved reference libraries taxonomic assignments, increased spatial and temporal sampling, and standardization of sampling technologies, wet lab processes, and bioinformatics pipelines (McClenaghan et al., 2020; Patin and Goodwin, 2022; Kelly et al., 2023).

5.2 Eukaryotic community structure is depth-dependent

Eukaryotic communities were depth-dependent with differing community composition for protists, invertebrates, and vertebrates (Figure 3). Protist community composition was highly influenced by depth with distinct communities at each of our sampled depths and a notable shift in dominant taxa between epipelagic and mesopelagic depth zones. Invertebrate communities were also depth-specific, although there was more overlap across the communities with samples clustering into three depth bands for the epipelagic (< 200 m), upper mesopelagic (300-500 m), and lower mesopelagic (> 500 m). Vertebrate communities were less structured with depth with samples at 500 m exhibiting a significant difference between epipelagic and lower mesopelagic samples. Depth-dependency of eukaryotic communities, especially for protists, has been established previously, with a distinct transition in community composition between the sunlit surface and the deep (Ollison et al., 2021; Blanco-Bercial et al., 2022; Yeh and Fuhrman, 2022; Sun et al., 2023; Anderson et al., 2024). For protists, a high relative abundance of photosynthetic

568 taxa including stramenopiles and chlorophytes transitions into dominance by alveolates,
569 especially Syndiniales and radiolarians.

570 Similar to other metazoan studies, we found high relative abundance of calanoid copepods
571 (Order Calanoida) in the water column, as well as a subsurface abundance of Siphonophorae
572 and Ctenophora (e.g., comb jellies) (Laroche et al., 2020b; Govindarajan et al., 2021). For
573 vertebrates, we detected high relative abundance of mesopelagic fish from families Myctophidae
574 and Gonostomatidae, which were also present in other metabarcoding studies (Canals et al.,
575 2021; Govindarajan et al., 2023b; Dan et al., 2024). In epipelagic waters, additional taxa occurred
576 in high relative abundance including the families Serrivomeridae (sawtooth eels), Molidae (molas),
577 and Alepocephalidae (slickheads).

578 The eukaryotic community at each depth was further shaped by a combination of unique,
579 shared, and cosmopolitan ASVs (Supplementary Figure S8). The detection of unique ASVs could
580 indicate niche specialization to different environmental conditions within a given taxonomic group
581 (Ollison et al., 2021; Anderson et al., 2024). Unexpectedly, we found unique ASVs for diatoms
582 and chlorophytes in deep waters. Rather than niche specialization of these photosynthetic taxa
583 to aphotic conditions, we hypothesize that these sequences indicate export of primary producers
584 out of the euphotic zone as sinking particles (Mestre et al., 2018; Durkin et al., 2022).

585 Animals shed DNA as they move through the water column, and we hypothesize that
586 unique ASVs represent cohorts of animals that are non-migratory while shared and cosmopolitan
587 ASVs reflect migratory cohorts. One possible explanation for the high occurrence of unique
588 invertebrate and vertebrate ASVs may be due to under-sampling of metazoan biodiversity, which
589 tend to be patchily distributed in the water column. Environmental factors that influence eDNA
590 shedding, persistence, and transport in combination with low-volume (~1-5 L) sampling efforts
591 impact eDNA recovery for metazoan detection (Govindarajan et al., 2022, 2023a). While these
592 volumes may be adequate for microbial studies, they likely underestimate metazoan biodiversity
593 in deep sea ecosystems (Govindarajan et al., 2022), which can lead to a skewed perspective of

their vertical and horizontal distribution. However, unique and cosmopolitan ASVs can be used to probe DVM behaviors, which may be useful to better understand the ecology of these otherwise elusive taxa that warrant further study.

We detected invertebrate and vertebrate ASVs that appeared at multiple sampling depths (shared and cosmopolitan ASVs), which included representatives from known migratory invertebrate taxa including copepods, cnidarians, and tunicates (Bianchi and Mislan, 2016; Romero-Romero et al., 2019; Easson et al., 2020), as well as mesopelagic fish including lanternfish and bristlemouths. Most of these fish are considered migratory except for *Cyclothone microdon* (bristlemouth) and *Scopeloberyx opisthopterus* (bigscale), which are lower mesopelagic and bathypelagic dwelling (Sutton, 2013; Govindarajan et al., 2023b; Richards et al., 2023). However, our study detected one ASV each of *C. microdon* (15 ASVs total) and *S. opisthopterus* (97 ASVs total) with a relatively high abundance in epipelagic waters, especially during the day. While studies have indicated that juvenile stages of mesopelagic fish may occur at shallower depths (Olivar and Beckley, 2022), it remains unclear whether the driving mechanism is ontogenetic migration or other drivers such as niche expansion that require further study (Sutton et al., 2008; Cook et al., 2013; Granata et al., 2023).

5.3 Protists increase ecosystem complexity and stability

Diversity (nodes or ASVs), connectivity (edges or interactions) and edge density (edge-to-node ratio) are core determinants of network complexity (Landi et al., 2018; Espinoza et al., 2020). Increasing biological diversity and their interactions increase ecosystem complexity, which often correlates with enhanced stability or resilience (McCann, 2000; Dunne et al., 2002; Carpentier et al., 2021; Nauta and De Domenico, 2024). Our ecological network analyses from multi-marker metabarcoding of the eukaryotic community showed that protistan taxa play a key role in mediating trophic interactions and ecosystem function. While metazoan networks were fragmented, the addition of protistan ASVs increased diversity and interactions (Supplementary

620 Table S7), producing fully connected networks at all depths with protist nodes facilitating
621 interactions between previously unconnected metazoan nodes (Figure 5). Increased protistan
622 diversity may stabilize connectivity by enhancing the likelihood that biological communities are
623 resilient to environmental fluctuations and can compensate the loss of functionally important taxa
624 (functional redundancy) (Naeem and Li, 1997; Naeem, 1998; McCann, 2000).

625 Alternatively, our fragmented ecological networks may reflect the more heterogenous
626 distributions of metazoan taxa that reduce co-occurrences and interactions, especially in the vast
627 and deep pelagic ocean where food is scarce (Robison, 2004; Ramirez-Llodra et al., 2010).
628 Fragmented networks may also reflect sampling biases associated with low-volume samples,
629 which may not provide a comprehensive snapshot of metazoan diversity and distribution
630 compared to more easily sampled protistan taxa (Anderson and Thompson, 2022; Govindarajan
631 et al., 2022). Significant knowledge gaps on metazoan eDNA further complicate our interpretation
632 of metazoan eDNA signatures due in part to unknown rates of DNA shedding across different
633 taxa and the varying impacts of environmental parameters on eDNA persistence (Allan et al.,
634 2021a, 2021b; McCartin et al., 2022; Govindarajan et al., 2023a). Nevertheless, molecular tools
635 like multi-marker metabarcoding and increasing availability of large-volume autonomous
636 samplers are revolutionizing biodiversity research and provide important multi-trophic insights that
637 are otherwise difficult to obtain, especially in the deep sea (Govindarajan et al., 2023a; Dan et al.,
638 2024; Haddock and Choy, 2024; Yang et al., 2024).

639

640 **5.4 Protists are key mediators of ecological interactions**

641 Positive interactions represent putative mutualistic or commensal relationships while
642 negative interactions reflect antagonistic relationships including competition, predation, and
643 parasitism (Landi et al., 2018). The balance of positive and negative interactions shapes
644 community interactions and ecosystem processes and in turn, ecological stability and resilience
645 to environmental change (Travis et al., 2005; Losapio et al., 2021). In our networks, there were

646 more positive interactions than negative interactions across all depth zones (Supplementary
647 Table S8), indicating an important role for mutualistic or facilitative relationships in marine
648 communities (Stachowicz, 2001; Deutschmann et al., 2024). The proportion of negative
649 interactions increased with depth, suggesting that competition or predation dynamics may
650 increase in importance in the relatively resource-scarce mesopelagic.

651 Positive networks were also more robust to node loss than negative networks and for both
652 network types, mesopelagic networks were more robust (Supplementary Figure S12). This may
653 be a result of the higher complexity found in the positive networks that can enhance network
654 stability. Moreover, positive networks had higher modularity, suggesting increased
655 compartmentalization of ASVs with potential niche partitioning and functional specialists
656 (Supplementary Table S8), which may also have a moderately stabilizing effect on networks. This
657 trend did not apply to depth-specific networks where positive and negative networks in the
658 epipelagic had higher modularity but lower robustness than mesopelagic networks. In our study,
659 decreased complexity in the epipelagic relative to mesopelagic depths is likely a stronger driver
660 of network stability. These dynamics suggest that negative-type interactions (e.g., key predator-
661 prey relationships), particularly in the epipelagic, may be more vulnerable to fragmentation or loss
662 of keystone taxa.

663 Top-ranking nodes indicating keystone taxa are highly connected ASVs that are important
664 facilitators of resource transfer (i.e., carbon and energy) throughout a network. A majority of the
665 top-ranking nodes in our study were protists (Supplementary Figures S14-S15), which included a
666 high number of ASVs belonging to the marine alveolate Syndiniales, suggesting an important role
667 for parasitism in the marine environment (Guillou et al., 2008; de Vargas et al., 2015; Anderson
668 et al., 2024). Copepod ASVs as well as various gelatinous taxa (cnidarians, ctenophores, and
669 salps), mesopelagic fish, and top predators (such as Risso's dolphin and common dolphinfish)
670 were also identified as keystone taxa (Supplementary Figures S14-15). Our findings highlight

protists as keystone taxa while also underscoring the importance of maintaining biodiversity across trophic levels and functional groups to sustain ecosystem function and stability.

We identified known and previously unobserved trophic interactions in our simplified food web analysis that featured protist associations with both invertebrates and vertebrates (Figure 6). Protist-based associations were more common than invertebrate-vertebrate associations and likely play a key role in carbon export out of the surface ocean and through deep sea food webs. For example, sinking particles and marine snow harbor microbial communities comprised of senescent primary producers and diverse microbial communities. Thus, our finding of protist-dominated interactions, especially in mesopelagic networks, aligns with the consensus that marine snow is an important food source in the deep sea (Dilling and Brzezinski, 2004; Choy et al., 2015; Cawley et al., 2021). Additionally, these putative interactions may not reflect direct feeding relationships between protists and metazoans, but rather highlight trophic dynamics in the environment that contribute to overall ecosystem function and warrant further study (Djurhuus et al., 2020; Holman et al., 2021)

6. Conclusions

Mesopelagic studies that integrate both microorganisms and metazoans are rare, yet growing anthropogenic pressures underscore the need for more holistic research on this critical ocean realm. Our study applied a multi-marker metabarcoding approach to survey mesopelagic biodiversity in the Northwest Atlantic Slope Water region and construct ecological networks to examine mesopelagic diversity, organismal interactions, and ecosystem stability. Our findings revealed depth-specific structuring of the eukaryotic community, spanning protists, invertebrates, and vertebrates. Notably, ecological networks that included all eukaryotic groups were more robust than metazoan-only networks, with the incorporation of protist ASVs enhancing network complexity and stability. The higher diversity of protistan ASVs likely conferred resilience to taxa loss across mesopelagic networks compared to the epipelagic network.

Additionally, we found that negative trophic interactions were more vulnerable to taxa loss than positive interactions, with implications for carbon and energy transfer within food webs and deep-sea carbon sequestration. While mesopelagic networks appear more structurally stable, it is crucial to recognize that surface and deep-sea ecosystems are intrinsically linked through the biological carbon pump and vertically migrating organisms. Therefore, a more complete understanding of biodiversity, species interactions, and their impact on ecosystem function across spatial, temporal, and taxonomic scales is essential for effective mesopelagic conservation and resource management. Future work incorporating a cross-domain lens, inclusive of bacteria and archaea, and biogeochemical processes such as carbon flux (Guidi et al., 2016; Nguyen et al., 2022; McMonagle et al., 2024) will help us better understand the role of biodiversity and their interactions in facilitating carbon cycling and other critical ecosystem services.

7. References

Aitchson, J. (1986). *The statistical analysis of compositional data*., 1986th Edn. London, England: Chapman and Hall.

Aksnes, D. L., Røstad, A., Kaartvedt, S., Martinez, U., Duarte, C. M., and Irigoien, X. (2017). Light penetration structures the deep acoustic scattering layers in the global ocean. *Sci Adv* 3, e1602468.

Allan, E. A., DiBenedetto, M. H., Lavery, A. C., Govindarajan, A. F., and Zhang, W. G. (2021a). Modeling characterization of the vertical and temporal variability of environmental DNA in the mesopelagic ocean. *Sci. Rep.* 11, 21273.

Allan, E. A., Zhang, W. G., Lavery, A., and Govindarajan, A. (2021b). Environmental DNA shedding and decay rates from diverse animal forms and thermal regimes. *Environ. DNA* 3, 492–514.

Amaral-Zettler, L. A., McCliment, E. A., Ducklow, H. W., and Huse, S. M. (2009). A method for studying protistan diversity using massively parallel sequencing of V9 hypervariable regions of small-subunit ribosomal RNA genes. *PLoS One* 4, e6372.

Amon, D. J., Rotjan, R. D., Kennedy, B. R. C., Alleng, G., Anta, R., Aram, E., et al. (2022). My Deep Sea, My Backyard: a pilot study to build capacity for global deep-ocean exploration and research. *Philos. Trans. R. Soc. Lond. B Biol. Sci.* 377, 20210121.

Anderson, S. R., Blanco-Bercial, L., Carlson, C. A., and Harvey, E. L. (2024). Role of Syndiniales parasites in depth-specific networks and carbon flux in the oligotrophic ocean. *ISME Commun* 4, ycae014.

Anderson, S. R., and Thompson, L. R. (2022). Optimizing an enclosed bead beating extraction method for microbial and fish environmental DNA. *Environ. DNA* 4, 291–303.

Arbizu, P. M. (2020). *pairwiseAdonis: Pairwise multilevel comparison using adonis. R package version 0.4*. Available at: https://github.com/pmartinezarbizu/pairwiseAdonis

Arístegui, J., Gasol, J. M., Duarte, C. M., and Herndld, G. J. (2009). Microbial oceanography of the dark ocean's pelagic realm. *Limnol. Oceanogr.* 54, 1501–1529.

Barham, E. G. (1966). Deep scattering layer migration and composition: observations from a diving saucer. *Science* 151, 1399–1403.

Bastiaanssen, T. F. S., Quinn, T. P., and Loughman, A. (2022). Bugs as features (part I): Concepts and foundations for the compositional data analysis of the microbiome-gut-brain axis. *arXiv [q-bio.GN]*. doi: 10.1038/s44220-023-00148-3

Bianchi, D., and Mislan, K. A. S. (2016). Global patterns of diel vertical migration times and velocities from acoustic data. *Limnol. Oceanogr.* 61, 353–364.

Bisson, K., McMonagle, H., Iglesias, I., Halfter, S., and Gallo, N. (2023). Five reasons to take the precautionary approach to deep sea exploitation. *Communications Earth & Environment* 4, 1–3.

Blanco-Bercial, L., Parsons, R., Bolaños, L. M., Johnson, R., Giovannoni, S. J., and Curry, R. (2022). The protist community traces seasonality and mesoscale hydrographic features in the oligotrophic Sargasso Sea. *Frontiers in Marine Science* 9. doi: 10.3389/fmars.2022.897140

Bolyen, E., Rideout, J. R., Dillon, M. R., Bokulich, N. A., Abnet, C. C., Al-Ghalith, G. A., et al. (2019). Reproducible, interactive, scalable and extensible microbiome data science using QIIME 2. *Nat. Biotechnol.* 37, 852–857.

Braun, C. D., Della Penna, A., Arostegui, M. C., Afonso, P., Berumen, M. L., Block, B. A., et al. (2023). Linking vertical movements of large pelagic predators with distribution patterns of biomass in the open ocean. *Proc. Natl. Acad. Sci. U. S. A.* 120, e2306357120.

Buesseler, K. O., Boyd, P. W., Black, E. E., and Siegel, D. A. (2020). Metrics that matter for assessing the ocean biological carbon pump. *Proc. Natl. Acad. Sci. U. S. A.* 117, 9679–9687.

Callahan, B. J., McMurdie, P. J., Rosen, M. J., Han, A. W., Johnson, A. J. A., and Holmes, S. P. (2016). DADA2: High-resolution sample inference from Illumina amplicon data. *Nat. Methods* 13, 581–583.

Canals, O., Mendibil, I., Santos, M., Irigoien, X., and Rodríguez-Ezpeleta, N. (2021). Vertical stratification of environmental DNA in the open ocean captures ecological patterns and behavior of deep-sea fishes. *Limnology and Oceanography Letters* 6, 339–347.

Carpentier, C., Barabás, G., Spaak, J. W., and De Laender, F. (2021). Reinterpreting the relationship between number of species and number of links connects community structure and stability. *Nat Ecol Evol* 5, 1102–1109.

Cavan, E. L., Laurenceau-Cornec, E. C., Bressac, M., and Boyd, P. W. (2019). Exploring the ecology of the mesopelagic biological pump. *Prog. Oceanogr.* 176, 102125.

Cawley, G. F., Décima, M., Mast, A., and Prairie, J. C. (2021). The effect of phytoplankton properties on the ingestion of marine snow by Calanus pacificus. *J. Plankton Res.* 43, 957–973.

Chavez, F., Min, M., Pitz, K., Truelove, N., Baker, J., LaScala-Grunewald, D., et al. (2021). Observing life in the sea using environmental DNA. *Oceanography* 34, 102–119.

Choy, C. A., Popp, B. N., Hannides, C. C. S., and Drazen, J. C. (2015). Trophic structure and food resources of epipelagic and mesopelagic fishes in the North Pacific Subtropical Gyre ecosystem inferred from nitrogen isotopic compositions. *Limnol. Oceanogr.* 60, 1156–1171.

Coenen, A. R., Hu, S. K., Luo, E., Muratore, D., and Weitz, J. S. (2020). A Primer for Microbiome Time-Series Analysis. *Front. Genet.* 11, 310.

Cook, A. B., Sutton, T. T., Galbraith, J. K., and Vecchione, M. (2013). Deep-pelagic (0–3000m) fish assemblage structure over the Mid-Atlantic Ridge in the area of the Charlie-Gibbs Fracture Zone. *Deep Sea Res. Part 2 Top. Stud. Oceanogr.* 98, 279–291.

Costello, M. J., and Chaudhary, C. (2017). Marine Biodiversity, Biogeography, Deep-Sea Gradients, and Conservation. *Curr. Biol.* 27, R511–R527.

Csárdi, G., and Nepusz, T. (2006). The igraph software package for complex network research. Available at: https://www.semanticscholar.org/paper/1d2744b83519657f5f2610698a8ddd177ced4f5c (Accessed July 14, 2024).

Dan, M. E., Portner, E. J., Bowman, J. S., Semmens, B. X., Owens, S. M., Greenwald, S. M., et al. (2024). Using low volume eDNA methods to sample pelagic marine animal assemblages. *PLoS One* 19, e0303263.

Davis, N. M., Proctor, D. M., Holmes, S. P., Relman, D. A., and Callahan, B. J. (2018). Simple statistical identification and removal of contaminant sequences in marker-gene and metagenomics data. *Microbiome* 6, 226.

de Vargas, C., Audic, S., Henry, N., Decelle, J., Mahé, F., Logares, R., et al. (2015). Ocean plankton. Eukaryotic plankton diversity in the sunlit ocean. *Science* 348, 1261605.

Décima, M., Stukel, M. R., Nodder, S. D., Gutiérrez-Rodríguez, A., Selph, K. E., Dos Santos, A. L., et al. (2023). Salp blooms drive strong increases in passive carbon export in the Southern Ocean. *Nat. Commun.* 14, 425.

Deutschmann, I. M., Delage, E., Giner, C. R., Sebastián, M., Poulain, J., Arístegui, J., et al. (2024). Disentangling microbial networks across pelagic zones in the tropical and subtropical global ocean. *Nat. Commun.* 15, 126.

Dilling, L., and Brzezinski, M. A. (2004). Quantifying marine snow as a food choice for zooplankton using stable silicon isotope tracers. *J. Plankton Res.* 26, 1105–1114.

Djurhuus, A., Closek, C. J., Kelly, R. P., Pitz, K. J., Michisaki, R. P., Starks, H. A., et al. (2020). Environmental DNA reveals seasonal shifts and potential interactions in a marine community. *Nat. Commun.* 11, 254.

Drazen, J. C., Smith, C. R., Gjerde, K. M., Haddock, S. H. D., Carter, G. S., Choy, C. A., et al. (2020). Midwater ecosystems must be considered when evaluating environmental risks of deep-sea mining. *Proceedings of the National Academy of Sciences* 117, 17455–17460.

Dunne, J. A., Williams, R. J., and Martinez, N. D. (2002). Network structure and biodiversity loss in food webs: robustness increases with connectance. *Ecol. Lett.* 5, 558–567.

Durkin, C. A., Cetinić, I., Estapa, M., Ljubešić, Z., Mucko, M., Neeley, A., et al. (2022). Tracing the path of carbon export in the ocean though DNA sequencing of individual sinking particles. *ISME J.* 16, 1896–1906.

Easson, C. G., Boswell, K. M., Tucker, N., Warren, J. D., and Lopez, J. V. (2020). Combined eDNA and Acoustic Analysis Reflects Diel Vertical Migration of Mixed Consortia in the Gulf of Mexico. *Frontiers in Marine Science* 7. doi: 10.3389/fmars.2020.00552

Espinoza, J. L., Shah, N., Singh, S., Nelson, K. E., and Dupont, C. L. (2020). Applications of weighted association networks applied to compositional data in biology. *Environ. Microbiol.* 22, 3020–3038.

Giering, S. L. C., Sanders, R., Lampitt, R. S., Anderson, T. R., Tamburini, C., Boutrif, M., et al. (2014). Reconciliation of the carbon budget in the ocean's twilight zone. *Nature* 507, 480–483.

Giner, C. R., Pernice, M. C., Balagué, V., Duarte, C. M., Gasol, J. M., Logares, R., et al. (2020). Marked changes in diversity and relative activity of picoeukaryotes with depth in the world ocean. *ISME J.* 14, 437–449.

Gold, Z., Sprague, J., Kushner, D. J., Zerecero Marin, E., and Barber, P. H. (2021). eDNA metabarcoding as a biomonitoring tool for marine protected areas. *PLoS One* 16, e0238557.

González, C. E., Blanco-Bercial, L., Escribano, R., Fernández-Urruzola, I., Rivera, R., and Ulloa, O. (2023). Revealing zooplankton diversity in the midnight zone. *Frontiers in Marine Science* 10. doi: 10.3389/fmars.2023.1252535

Govindarajan, A. F., Adams, A., Allan, E., Herrera, S., Lavery, A., Llopiz, J., et al. (2023a). Advances in environmental DNA sampling for observing ocean twilight zone animal diversity. *Oceanography*. doi: 10.5670/oceanog.2023.s1.27

Govindarajan, A. F., Francolini, R. D., Jech, J. M., Lavery, A. C., Llopiz, J. K., Wiebe, P. H., et al. (2021). Exploring the Use of Environmental DNA (eDNA) to Detect Animal Taxa in the Mesopelagic Zone. *Frontiers in Ecology and Evolution* 9. doi: 10.3389/fevo.2021.574877

Govindarajan, A. F., Llopiz, J. K., Caiger, P. E., Jech, J. M., Lavery, A. C., McMonagle, H., et al. (2023b). Assessing mesopelagic fish diversity and diel vertical migration with environmental DNA. *Frontiers in Marine Science* 10. doi: 10.3389/fmars.2023.1219993

Govindarajan, A. F., McCartin, L., Adams, A., Allan, E., Belani, A., Francolini, R., et al. (2022). Improved biodiversity detection using a large-volume environmental DNA sampler with in situ filtration and implications for marine eDNA sampling strategies. *Deep Sea Res. Part I* 189, 103871.

Granata, A., Bergamasco, A., Zagami, G., Guglielmo, R., Bonanzinga, V., Minutoli, R., et al. (2023). Daily vertical distribution and diet of Cyclothone braueri (Gonostomatidae) in the Polcevera submarine canyon (Ligurian Sea, north-western Mediterranean). *Deep Sea Res. Part I* 199, 104113.

Groeneveld, J., Berger, U., Henschke, N., Pakhomov, E. A., Reiss, C. S., and Meyer, B. (2020). Blooms of a key grazer in the Southern Ocean – An individual-based model of Salpa thompsoni. *Prog. Oceanogr.* 185, 102339.

Guidi, L., Chaffron, S., Bittner, L., Eveillard, D., Larhlimi, A., Roux, S., et al. (2016). Plankton networks driving carbon export in the oligotrophic ocean. *Nature* 532, 465–470.

Guillou, L., Bachar, D., Audic, S., Bass, D., Berney, C., Bittner, L., et al. (2013). The Protist Ribosomal Reference database (PR2): a catalog of unicellular eukaryote small sub-unit rRNA sequences with curated taxonomy. *Nucleic Acids Res.* 41, D597-604.

Guillou, L., Viprey, M., Chambouvet, A., Welsh, R. M., Kirkham, A. R., Massana, R., et al. (2008). Widespread occurrence and genetic diversity of marine parasitoids belonging to Syndiniales (Alveolata). *Environ. Microbiol.* 10, 3349–3365.

Haddock, S. H. D., and Choy, C. A. (2024). Life in the Midwater: The Ecology of Deep Pelagic Animals. *Ann. Rev. Mar. Sci.* 16, 383–416.

Hemsley, V., Füssel, J., Duret, M. T., Rayne, R. R., Iversen, M. H., Henson, S. A., et al. (2023). Suspended particles are hotspots of microbial remineralization in the ocean's twilight zone. *Deep Sea Res. Part 2 Top. Stud. Oceanogr.* 212, 105339.

Herndl, G. J., and Reinthaler, T. (2013). Microbial control of the dark end of the biological pump. *Nat. Geosci.* 6, 718–724.

Holman, L. E., de Bruyn, M., Creer, S., Carvalho, G., Robidart, J., and Rius, M. (2021). Animals, protists and bacteria share marine biogeographic patterns. *Nat Ecol Evol* 5, 738–746.

Iglesias, I. S., Santora, J. A., Fiechter, J., and Field, J. C. (2023). Mesopelagic fishes are important prey for a diversity of predators. *Frontiers in Marine Science* 10. doi: 10.3389/fmars.2023.1220088

Iyer, S., Killingback, T., Sundaram, B., and Wang, Z. (2013). Attack robustness and centrality of complex networks. *PLoS One* 8, e59613.

Jousset, A., Bienhold, C., Chatzinotas, A., Gallien, L., Gobet, A., Kurm, V., et al. (2017). Where less may be more: how the rare biosphere pulls ecosystems strings. *ISME J.* 11, 853–862.

Kaartvedt, S., Staby, A., and Aksnes, D. L. (2012). Efficient trawl avoidance by mesopelagic fishes causes large underestimation of their biomass. *Mar. Ecol. Prog. Ser.* 456, 1–6.

Kelly, R. P., Lodge, D. M., Lee, K. N., Theroux, S., Sepulveda, A. J., Scholin, C. A., et al. (2023). Toward a national eDNA strategy for the United States. *Environ. DNA*. doi: 10.1002/edn3.432

Kurtz, Z. D., Müller, C. L., Miraldi, E. R., Littman, D. R., Blaser, M. J., and Bonneau, R. A. (2015). Sparse and compositionally robust inference of microbial ecological networks. *PLoS Comput. Biol.* 11, e1004226.

Landi, P., Minoarivelo, H. O., Brännström, Å., Hui, C., and Dieckmann, U. (2018). Complexity and stability of ecological networks: a review of the theory. *Popul. Ecol.* 60, 319–345.

Laroche, O., Kersten, O., Smith, C. R., and Goetze, E. (2020a). Environmental DNA surveys detect distinct metazoan communities across abyssal plains and seamounts in the western Clarion Clipperton Zone. *Mol. Ecol.* 29, 4588–4604.

Laroche, O., Kersten, O., Smith, C. R., and Goetze, E. (2020b). From Sea Surface to Seafloor: A Benthic Allochthonous eDNA Survey for the Abyssal Ocean. *Frontiers in Marine Science* 7. doi: 10.3389/fmars.2020.00682

Logares, R., Audic, S., Bass, D., Bittner, L., Boutte, C., Christen, R., et al. (2014). Patterns of rare and abundant marine microbial eukaryotes. *Curr. Biol.* 24, 813–821.

Losapio, G., Schöb, C., Staniczenko, P. P. A., Carrara, F., Palamara, G. M., De Moraes, C. M., et al. (2021). Network motifs involving both competition and facilitation predict biodiversity in alpine plant communities. *Proc. Natl. Acad. Sci. U. S. A.* 118. doi: 10.1073/pnas.2005759118

Lynch, M. D. J., and Neufeld, J. D. (2015). Ecology and exploration of the rare biosphere. *Nat. Rev. Microbiol.* 13, 217–229.

Lyons, K. G., Brigham, C. A., Traut, B. H., and Schwartz, M. W. (2005). Rare species and ecosystem functioning: Rare species and ecosystem functioning. *Conserv. Biol.* 19, 1019–1024.

Madin, L. P., Kremer, P., Wiebe, P. H., Purcell, J. E., Horgan, E. H., and Nemazie, D. A. (2006). Periodic swarms of the salp Salpa aspera in the Slope Water off the NE United States: Biovolume, vertical migration, grazing, and vertical flux. *Deep Sea Res. Part 1 Oceanogr. Res. Pap.* 53, 804–819.

Martin, A., Boyd, P., Buesseler, K., Cetinic, I., Claustre, H., Giering, S., et al. (2020). The oceans' twilight zone must be studied now, before it is too late. *Nature Publishing Group UK*. doi: 10.1038/d41586-020-00915-7

Martin, M. (2011). Cutadapt removes adapter sequences from high-throughput sequencing reads. *EMBnet J.* 17, 10.

Matthews, S. A., and Blanco-Bercial, L. (2023). Divergent patterns of zooplankton connectivity in the epipelagic and mesopelagic zones of the eastern North Pacific. *Ecol. Evol.* 13, e10664.

Mazuecos, I. P., Arístegui, J., Vázquez-Domínguez, E., Ortega-Retuerta, E., Gasol, J. M., and Reche, I. (2015). Temperature control of microbial respiration and growth efficiency in the mesopelagic zone of the South Atlantic and Indian Oceans. *Deep Sea Res. Part I* 95, 131–138.

McCann, K. S. (2000). The diversity-stability debate. *Nature* 405, 228–233.

McCartin, L. J., Vohsen, S. A., Ambrose, S. W., Layden, M., McFadden, C. S., Cordes, E. E., et al. (2022). Temperature Controls eDNA Persistence across Physicochemical Conditions in Seawater. *Environ. Sci. Technol.* 56, 8629–8639.

McClenaghan, B., Fahner, N., Cote, D., Chawarski, J., McCarthy, A., Rajabi, H., et al. (2020). Harnessing the power of eDNA metabarcoding for the detection of deep-sea fishes. *PLoS One* 15, e0236540.

McMonagle, H., Llopiz, J. K., Maas, A. E., Steinberg, D. K., Govindarajan, A. F., and Essington, T. E. (2024). Quantifying uncertainty in the contribution of mesopelagic fishes to the biological carbon pump in the Northeast Atlantic Ocean. *ICES J. Mar. Sci.* 81, 2037–2051.

McMurdie, P. J., and Holmes, S. (2013). phyloseq: an R package for reproducible interactive analysis and graphics of microbiome census data. *PLoS One* 8, e61217.

Mestre, M., Ruiz-González, C., Logares, R., Duarte, C. M., Gasol, J. M., and Sala, M. M. (2018). Sinking particles promote vertical connectivity in the ocean microbiome. *Proc. Natl. Acad. Sci. U. S. A.* 115, E6799–E6807.

Miya, M., Sato, Y., Fukunaga, T., Sado, T., Poulsen, J. Y., Sato, K., et al. (2015). MiFish, a set of universal PCR primers for metabarcoding environmental DNA from fishes: detection of more than 230 subtropical marine species. *R Soc Open Sci* 2, 150088.

Mouillot, D., Bellwood, D. R., Baraloto, C., Chave, J., Galzin, R., Harmelin-Vivien, M., et al. (2013). Rare species support vulnerable functions in high-diversity ecosystems. *PLoS Biol.* 11, e1001569.

Naeem, S. (1998). Species redundancy and ecosystem reliability. *Conserv. Biol.* 12, 39–45.

Naeem, S., and Li, S. (1997). Biodiversity enhances ecosystem reliability. *Nature* 390, 507–509.

Nauta, J., and De Domenico, M. (2024). Topological conditions drive stability in meta-ecosystems. *Phys. Rev. Res.* 6, 043055.

Nguyen, T. T. H., Zakem, E. J., Ebrahimi, A., Schwartzman, J., Caglar, T., Amarnath, K., et al. (2022). Microbes contribute to setting the ocean carbon flux by altering the fate of sinking particulates. *Nat. Commun.* 13, 1657.

O'Brien, T. D., Blanco-Bercial, L., Questel, J. M., Batta-Lona, P. G., and Bucklin, A. (2024). "MetaZooGene Atlas and Database: Reference Sequences for Marine Ecosystems," in *DNA Barcoding: Methods and Protocols*, ed. R. DeSalle (New York, NY: Springer US), 475–489.

Oksanen, J., Simpson, G., Blanchet, F., Kindt, R., Legendre, P., Minchin, P., et al. (2022). vegan: Community Ecology Package. R package version 2.6-4. Available at: https://CRAN.R-project.org/package=vegan

Olivar, M. P., and Beckley, L. E. (2022). Vertical distribution patterns of early stages of mesopelagic fishes along 110 °E, south-east Indian Ocean. *Deep Sea Res. Part 2 Top. Stud. Oceanogr.* 201, 105111.

Oliver, T. H., Heard, M. S., Isaac, N. J. B., Roy, D. B., Procter, D., Eigenbrod, F., et al. (2015). Biodiversity and Resilience of Ecosystem Functions. *Trends Ecol. Evol.* 30, 673–684.

Ollison, G. A., Hu, S. K., Mesrop, L. Y., DeLong, E. F., and Caron, D. A. (2021). Come rain or shine: Depth not season shapes the active protistan community at station ALOHA in the North Pacific Subtropical Gyre. *Deep Sea Res. Part I* 170, 103494.

Paffenhöfer, G.-A., Atkinson, L. P., Lee, T. N., Verity, P. G., and Bulluck, L. R., III (1995). Distribution and abundance of thaliaceans and copepods off the southeastern U.S.A. during winter. *Cont. Shelf Res.* 15, 255–280.

Patin, N. V., and Goodwin, K. D. (2022). Capturing marine microbiomes and environmental DNA: A field sampling guide. *Front. Microbiol.* 13, 1026596.

Pedregosa, F., Varoquaux, G., Gramfort, A., Michel, V., Thirion, B., Grisel, O., et al. (2011). Scikit-learn: Machine Learning in Python. *J. Mach. Learn. Res.* abs/1201.0490, 2825–2830.

Perissinotto, R., and A. Pakhomov, E. (1998). The trophic role of the tunicate Salpa thompsoni in the Antarctic marine ecosystem. *J. Mar. Syst.* 17, 361–374.

Pitz, K., Truelove, N., Nye, C., Michisaki, R. P., and Chavez, F. (2020). Environmental DNA (eDNA) 12S Metabarcoding Illumina MiSeq NGS PCR Protocol (Touchdown). Available at: https://www.protocols.io/view/environmental-dna-edna-12s-metabarcoding-illumina-kqdg35kqzv25/v2?step=6 (Accessed October 24, 2023).

Pruesse, E., Quast, C., Knittel, K., Fuchs, B. M., Ludwig, W., Peplies, J., et al. (2007). SILVA: a comprehensive online resource for quality checked and aligned ribosomal RNA sequence data compatible with ARB. *Nucleic Acids Res.* 35, 7188–7196.

Quast, C., Pruesse, E., Yilmaz, P., Gerken, J., Schweer, T., Yarza, P., et al. (2013). The SILVA ribosomal RNA gene database project: improved data processing and web-based tools. *Nucleic Acids Res.* 41, D590-6.

Ramirez-Llodra, E., Brandt, A., Danovaro, R., De Mol, B., Escobar, E., German, C. R., et al. (2010). Deep, diverse and definitely different: unique attributes of the world's largest ecosystem. *Biogeosciences* 7, 2851–2899.

Richards, T. M., Sutton, T. T., Woodstock, M. S., Judkins, H., and David Wells, R. J. (2023). Body size, depth of occurrence, and local oceanography shape trophic structure in a diverse deep-pelagic micronekton assemblage. *Prog. Oceanogr.* 213, 102998.

Robeson, M. S., 2nd, O'Rourke, D. R., Kaehler, B. D., Ziemski, M., Dillon, M. R., Foster, J. T., et al. (2021). RESCRIPt: Reproducible sequence taxonomy reference database management. *PLoS Comput. Biol.* 17, e1009581.

Robinson, C., Steinberg, D. K., Anderson, T. R., Arístegui, J., Carlson, C. A., Frost, J. R., et al. (2010). Mesopelagic zone ecology and biogeochemistry – a synthesis. *Deep Sea Res. Part 2 Top. Stud. Oceanogr.* 57, 1504–1518.

Robison, B. H. (2004). Deep pelagic biology. *J. Exp. Mar. Bio. Ecol.* 300, 253–272.

Romero-Romero, S., Choy, C. A., Hannides, C. C. S., Popp, B. N., and Drazen, J. C. (2019). Differences in the trophic ecology of micronekton driven by diel vertical migration. *Limnol. Oceanogr.* 64, 1473–1483.

Sala, E., Mayorga, J., Bradley, D., Cabral, R. B., Atwood, T. B., Auber, A., et al. (2021). Protecting the global ocean for biodiversity, food and climate. *Nature* 592, 397–402.

Schloss, P. D. (2024). Waste not, want not: revisiting the analysis that called into question the practice of rarefaction. *mSphere* 9, e0035523.

St. John, M. A., Borja, A., Chust, G., Heath, M., Grigorov, I., Mariani, P., et al. (2016). A Dark Hole in Our Understanding of Marine Ecosystems and Their Services: Perspectives from the Mesopelagic Community. *Frontiers in Marine Science* 3. doi: 10.3389/fmars.2016.00031

Stachowicz, J. J. (2001). Mutualism, facilitation, and the structure of ecological communities. *Bioscience* 51, 235.

Stukel, M. R., Décima, M., Selph, K. E., and Gutiérrez-Rodríguez, A. (2021). Size-specific grazing and competitive interactions between large salps and protistan grazers. *Limnol. Oceanogr.* 66, 2521–2534.

Suarez-Bregua, P., Álvarez-González, M., Parsons, K. M., Rotllant, J., Pierce, G. J., and Saavedra, C. (2022). Environmental DNA (eDNA) for monitoring marine mammals: Challenges and opportunities. *Frontiers in Marine Science* 9. doi: 10.3389/fmars.2022.987774

Sun, P., Wang, Y., Zhang, Y., Logares, R., Cheng, P., Xu, D., et al. (2023). From the Sunlit to the Aphotic Zone: Assembly Mechanisms and Co-Occurrence Patterns of Protistan-Bacterial Microbiotas in the Western Pacific Ocean. *mSystems* 8, e0001323.

Sutton, T. T. (2013). Vertical ecology of the pelagic ocean: classical patterns and new perspectives. *J. Fish Biol.* 83, 1508–1527.

Sutton, T. T., Clark, M. R., Dunn, D. C., Halpin, P. N., Rogers, A. D., Guinotte, J., et al. (2017). A global biogeographic classification of the mesopelagic zone. *Deep Sea Res. Part I* 126, 85–102.

Sutton, T. T., Porteiro, F. M., Heino, M., Byrkjedal, I., Langhelle, G., Anderson, C. I. H., et al. (2008). Vertical structure, biomass and topographic association of deep-pelagic fishes in relation to a mid-ocean ridge system. *Deep Sea Res. Part 2 Top. Stud. Oceanogr.* 55, 161–184.

Tipton, L., Müller, C. L., Kurtz, Z. D., Huang, L., Kleerup, E., Morris, A., et al. (2018). Fungi stabilize connectivity in the lung and skin microbial ecosystems. *Microbiome* 6, 12.

Tolochko, P., and Vadrot, A. B. M. (2021). The usual suspects? Distribution of collaboration capital in marine biodiversity research. *Mar. Policy* 124, 104318.

Travis, J. M. J., Brooker, R. W., and Dytham, C. (2005). The interplay of positive and negative species interactions across an environmental gradient: insights from an individual-based simulation model. *Biol. Lett.* 1, 5–8.

Tyner, S., Briatte, F., and Hofmann, H. (2017). Network visualization with ggplot2. *R J.* 9, 27.

Wickham, H. (2016). *Ggplot2: Elegant graphics for data analysis*., 2nd Edn. Cham, Switzerland: Springer International Publishing.

Wiebe, P. H., Madin, L. P., Haury, L. R., Harbison, G. R., and Philbin, L. M. (1979). Diel vertical migration bySalpa aspera and its potential for large-scale particulate organic matter transport to the deep-sea. *Mar. Biol.* 53, 249–255.

Willis, C., Gardner, K. G., Arostegui, M. C., Braun, C. D., Golet, W., Houghton, L., et al. (2025). Evaluating the importance of mesopelagic prey to three top teleost predators in the northwest Atlantic Ocean. *ICES J. Mar. Sci.* 82, fsaf028.

Yang, N., Jin, D., and Govindarajan, A. F. (2024). Applying environmental DNA approaches to inform marine biodiversity conservation: The case of the Ocean Twilight Zone. *Mar. Policy* 165, 106151.

Yeh, Y.-C., and Fuhrman, J. A. (2022). Contrasting diversity patterns of prokaryotes and protists over time and depth at the San-Pedro Ocean Time series. *ISME Communications* 2, 1–12.

Zeldis, J. R., Davis, C. S., James, M. R., Ballara, S. L., Booth, W. E., and Chang, F. H. (1995). Salp grazing:effects on phytoplankton abundance, vertical distribution and taxonomic composition in a coastal habitat. *Mar. Ecol. Prog. Ser.* 126, 267–283.